ICAS-98-1,2,1

A98-31447

THE SENSITIVITY OF SCT DESIGNS TO AIRFIELD NOISE REQUIREMENTS: AN INVESTIGATION USING MULTIVARIATE OPTIMISATION

Kevin P. Nicholls
British Aerospace Airbus, Bristol, United Kingdom

Carl A. Lee
Defence Evaluation & Research Agency, Farnborough, United Kingdom

Abstract

The ASTRO multivariate optimisation code, comprising Supersonic Commercial Transport (SCT) conceptual design synthesis routines linked to a constrained optimisation method, is briefly described. The code includes an airfield noise estimation method that allows constraints on noise to be applied as part of the design optimisation.

The results of a number of noise-related studies performed with ASTRO are presented. An optimum configuration that satisfies Stage 3 noise requirements is obtained, and its sensitivity to reductions in individual noise limits explored. A range of measures that may reduce noise are then investigated, comprising: increased glideslope angle, drag reductions at low-speed and cruise speeds, the use of flap systems and optimisation of initial climb speed. The net benefits of most of these measures are presented in terms of their effects on noise limit sensitivity curves.

Introduction

Any second generation Supersonic Commercial Transport (SCT) aircraft which intends to succeed in commercial service will have to meet a particularly challenging combination of performance goals to be viable. A crucial constraint is the need to meet the same airfield noise requirements that apply to modern subsonic airliners. Designing an SCT to meet current FAR36 Stage 3 noise requirements is already a demanding task, but these may be superseded by more stringent requirements within the timescale of a new SCT. Hence the ability of SCT designs to meet post-Stage 3 noise requirements is an important issue.

In developing an SCT concept it is very important to have tools that can find the best combination of design and technology parameters and hence produce a fully integrated solution. Central to such tools is constrained multivariate optimisation (MVO).

The Defence Evaluation & Research Agency (DERA) has considerable experience in the application of MVO to aircraft conceptual design for the purposes of assessing concepts, technologies and performance, and for sensitivity studies[1-3]. This experience is based on the use of a DERA-developed constrained non-linear optimisation method, in conjunction with design synthesis codes for various classes of aircraft. British Aerospace (BAe) has substantial experience of supersonic transport design from its Concorde involvement and has conceptual design methods which have been developed and updated during follow-on studies for any next generation SCT. DERA and BAe have collaborated on the development of an SCT design synthesis, with BAe methods being incorporated within DERA methodology, to produce the Advanced Supersonic TRansport Optimisation (ASTRO) MVO code for joint studies and further development.

This paper briefly describes the methods used within ASTRO, and the use and versatility of its MVO implementation. It then presents the results of a number of noise-related studies. Initially a baseline optimum configuration satisfying Stage 3 noise regulations is obtained, then the sensitivities of this solution to changes in individual noise limits are presented. From these sensitivity curves, key noise problems are identified, such as the difficulty the aircraft has in accommodating any reduction in the approach noise limit relative to its current Stage 3 value. The remainder of the paper comprises investigations of a number of potential noise reduction measures, such as increased approach glideslope angle, low-speed and cruise drag reductions, the use of trailing-edge and leading-edge flaps and optimisation of the initial climb speed after take-off.

The presented optimised solutions are minimum take-off mass configurations which satisfy a specified set of performance requirements, including specified noise limits that were applied under Stage 3 rules. A range of key design parameters were optimised, including parameters that determine the aircraft flight path between lift-off and the flyover noise measurement point. The use of noise limit sensitivity curves to present optimisation results allows the true net benefits of noise reduction measures to be illustrated.

21st ICAS Congress
13-18 September 1998
Melbourne, Australia

Multivariate Optimisation With RQPMIN

ASTRO comprises an SCT design synthesis linked to the RQPMIN optimisation code. RQPMIN finds the values of a set of independent variables which minimise the value of a function of those variables (the objective function), while simultaneously satisfying a set of constraints. For a given optimisation run, individual independent variables can either be fixed at their starting value or made available to RQPMIN to vary between their specified upper and lower bounds. Individual constraints can be switched on or off as required.

Currently there is a choice of 3 objective functions within ASTRO: maximum take-off mass, cash operating costs or direct operating costs. The code optimises up to 53 independent variables (e.g. engine scale, wing area) while applying up to 50 constraints (e.g. take-off distance, approach noise).

The ASTRO Design Synthesis

The SCT design synthesis performs all computations required to calculate the values of the objective and constraint functions that correspond to a set of independent variable values passed to it by RQPMIN. The design synthesis routines are typically called by RQPMIN several hundred times, but sometimes several thousand times, before converging to a solution. Since multiple runs are normally required to explore a problem fully, there is a requirement to limit the run time, and hence the complexity, of the synthesis.

The ASTRO synthesis is highly modular in structure with separate top level subroutines for individual disciplines, such as geometry synthesis, mass estimation, mission modelling, and low-speed performance modelling. Below these are layers of more specific functional subroutines, of which some such as the drag estimation routines contain several alternative methods that can be selected via input variables.

Aircraft Geometry

This has been kept as simple as possible while still representing SCT configurations of interest sufficiently well to allow useful MVO studies to be performed. Figure 1 shows a typical configuration used by ASTRO.

The fuselage. This consists of a cylindrical centre section with simple tapers of equal length at both ends. The cross-section for a given width and height can be anything between an ellipse and a rectangle, specified by a 'squareness factor', with consequent changes to cross-sectional and wetted areas. Local reduction in fuselage width for area-ruling can be applied to reduce aircraft maximum cross-sectional area and hence wave drag.

The wing. The wing planform has been simply defined with just two leading edge sweep angles and a single trailing edge sweep angle. Aerofoil shapes are specified either by using a combination of simple elliptic and power law expressions, fore and aft of maximum thickness respectively, or by using the expressions employed by Hutchison et al[4] which are based on the NACA 4-digit definition. The former method allows a trailing edge thickness to be specified and both methods include options for either round or sharp leading edges. Thickness/chord ratio is defined at three spanwise locations (root, tip and an 'intermediate' location) and interpolated between them. Leading and trailing edge high-lift devices of required sizes can also be modelled.

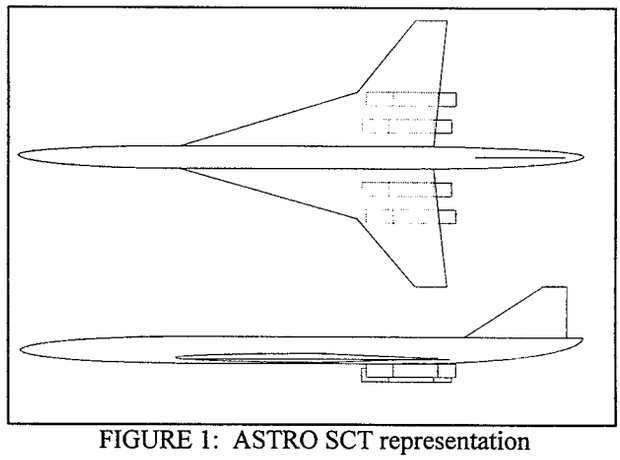

FIGURE 1: ASTRO SCT representation

The engines and nacelles. A set of performance data for a range of heights, Mach numbers and throttle settings as well as size and mass for a datum size engine is supplied as input. These data are scaled by functions of the engine thrust scale factor (an independent variable) to allow changes in engine size to be represented. Nacelle size is related to engine size via a further set of input parameters. The shape of the nacelle cross-section can be selected from four options, including a 'paired' Concorde style arrangement. Circular streamtubes are subtracted from the nacelle cross-sectional area when calculating the aircraft maximum cross-sectional area for wave drag estimation. Nacelle location on the wing is controlled by independent variables and constraints.

The fin. Although fin area is an independent variable there is currently no modelling in ASTRO to drive its size. Current studies therefore fix this value, along with the other input variables that determine fin shape.

Mass Estimation

Most of the mass estimation in ASTRO is based on simple BAe expressions which were developed with

Concorde experience and follow-on studies. A number have been updated recently to give improved agreement with more detailed methods for the SCT configurations of current interest. For example the wing mass expression in ASTRO now matches data from a buckling panel theory method with an average error of 2% across a range of wing areas from 650 to 930m^2 and aspect ratios from 1.7 to 2.6. Factors have been incorporated into the mass estimates of most components to allow mass reduction technologies relative to a datum to be easily represented and adjusted.

Drag Estimation

The drag of the complete aircraft is divided into skin friction drag, wave drag and lift-dependent drag for estimation purposes. Spillage drag is incorporated in the engine performance data supplied as input.

Skin friction drag. This is calculated using a DERA method which multiplies the wetted area of each major aircraft component by a mean turbulent skin friction coefficient of a flat plate of uniform roughness at a Reynolds number based on an appropriate component length. A component form factor is then applied. The resulting component drags are multiplied by individual technology factors which are supplied as inputs to allow the aerodynamic benefits of technologies such as laminar flow to be represented.

Wave drag. ASTRO currently contains two alternative wave drag methods that can be selected:

A BAe method uses fuselage and wing volume and an appropriate component length to estimate the drag of the aircraft with no engines, and then applies an engine installation factor. This method currently only achieves acceptable accuracy for a limited range of configurations and requires further development.

A method based on the approach of Raymer[5] is also included, which gives a wave drag proportional to $(S_{max}/L_{fus})^2$ where S_{max} is the maximum cross-sectional area of the aircraft and L_{fus} is the fuselage length. An efficiency factor is also applied which allows the method to be matched to measured data with a known level of area-ruling. Although the expression used is fairly simple the method requires a considerable amount of computation due to the need to search longitudinally for S_{max}, which includes contributions from the fuselage, wing and usually the engine nacelles. This search requires accurate estimation of aircraft cross-sectional area at a range of longitudinal positions, which in turn requires careful modelling of features such as the wing-fuselage junction. The advantage of the method is that it controls maximum aircraft cross-sectional area, a good first-order wave drag reduction strategy.

Lift-dependent drag. At subsonic Mach numbers lift-dependent drag is interpolated from arrays of BAe aerodynamic data for SCT wings which currently cover aspect ratios from 1.7 to 2.6. These data cover both subsonic cruise and low speed C_L ranges, and include drag changes due to the deflection of datum sized leading and trailing edge flaps. Simple scaling of the datum high-lift device data, based on flap area, is used to estimate the effects of alternative device sizes.

A BAe expression based on wing planform geometry is used for lift-dependent drag in supersonic cruise. This matches an array of results from a more sophisticated and computationally intensive linear theory method.

Mission Modelling

Mission definitions are input to ASTRO and constraints are used to ensure that the optimised aircraft can complete them. Currently a maximum of five separate missions can be used. Individual missions are defined as a series of cruise-climb legs of specified lengths and Mach numbers. The leg lengths are automatically adjusted by ASTRO to model the additional fuel used in changing height and speed between legs. The starting altitude of each leg is an independent variable, early experimentation showing that this freedom can result in considerable improvements in aircraft performance. One of the missions can be nominated as the economic mission for estimating operating costs.

Cost Estimation

ASTRO has the ability to calculate both cash and direct operating costs and use them as objective functions. Cash costs comprise the flying and maintenance costs whereas the direct operating costs include the additional financial costs to an airline of buying and owning the aircraft.

Noise Estimation

ASTRO uses a BAe jet noise prediction method, based on measured data for Concorde with Olympus engines but modified to simulate a more general powerplant without reheat. Adjustments to represent advances in jet pipe liners and the elimination of tones since Concorde have also been included. The method estimates the sideline, flyover and approach noise levels used for noise certification and requires engine thrust, jet velocity, jet pressure ratio and aircraft height at each flight condition of interest. The three engine parameters are interpolated from the input engine data file. The method has been validated against more sophisticated flyover and sideline noise predictions for current variable cycle engine concepts. Turbo-machinery and airframe noise are not currently calculated although they could become important if jet noise is sufficiently reduced.

An integral part of the noise estimation process is the modelling of the take-off and approach flight paths as shown in figure 2, in order to obtain aircraft heights and throttle settings at the noise certification conditions. The ASTRO model of the take-off flight path includes a noise abatement 'bunt' manoeuvre which allows the engines to be throttled back at a cutback height (an independent variable), to a setting that can maintain a specified minimum climb gradient.

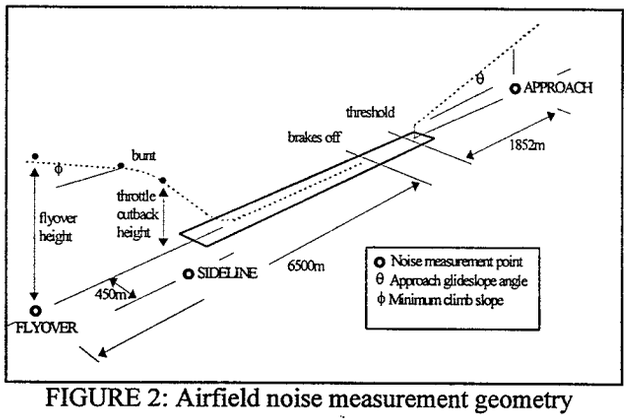

FIGURE 2: Airfield noise measurement geometry

The lower the aircraft, the shallower its angle above the ground when viewed from the sideline distance of 450m, which increases the ground attenuation of noise measured at the sideline distance. Hence a reduction in cutback height reduces the sideline noise. However, a lower cutback height also causes a reduction in the aircraft height above the flyover noise measurement point. This increases flyover noise since this is not dependent on ground attenuation effects. Since cutback height is an independent variable in ASTRO it can be used during optimisation as a means of trading sideline against flyover noise if required, to aid satisfaction of the complete set of noise constraints.

Noise Limit Sensitivity Study

ASTRO was used to perform a study which investigated the sensitivity of an SCT aircraft with Mid-Tandem Fan (MTF) engines to changes in airfield noise limits. A configuration that satisfies the Stage 3 noise limits was first optimised to provide a baseline aircraft. The noise limits were then reduced (i.e. made more severe) while retaining the same rules of application, the aircraft reoptimised, and the effects on the optimum configuration investigated.

Noise limit application. For certification, aircraft noise is measured in terms of effective perceived noise level (EPNdB) at the three locations shown in figure 2 corresponding to sideline, flyover and approach. The current FAR36 Stage 3 limits at these locations increase linearly with the logarithm of aircraft maximum take-off mass up to a given mass above which the noise limit is constant. These noise cut-offs occur at 400 tonnes for sideline, 386 tonnes for flyover and 280 tonnes for approach noise. It is important to note that the limits are not individual absolute limits, but are applied via the following Stage 3 rules:

1. *Any individual limit may be exceeded by a margin of up to 2 EPNdB,*
2. *The sum of the three margins (+ve for limit exceedance, -ve for limit satisfaction) must be zero or less,*
3. *The sum of all exceedance (+ve only) margins may not exceed 3 EPNdB.*

Hence it requires five constraints rather than three, to apply Stage 3 limits in ASTRO.

Study Assumptions

To perform the study it was necessary to identify a representative set of performance requirements for an SCT, decide which design parameters should be fixed and which should be optimised, and what technology levels would be appropriate. The optimised aircraft was required to achieve the following performance:

- *Accommodate 253 passengers in 6 abreast seating,*
- *Fly a range of 5700nm, of which the first 3700nm is flown at Mach 2.0 and the final 2000nm is flown at Mach 0.95, with a full passenger load,*
- *Fly a range of 5200nm, all at Mach 2.0, with a full passenger load,*
- *A maximum take-off distance of 3353m (11000ft),*
- *A maximum approach speed of 82.3m/s (160kts),*
- *A minimum 2nd segment climb gradient (with one engine-out) of 3%,*
- *A minimum climb capability in cruise of 2.54m/s (500ft/min),*
- *A minimum throttle cutback height of 150m,*
- *Meet Stage 3 (or stricter when specified) noise limits.*

The objective function to be minimised was the aircraft maximum take-off mass and the independent variables that were optimised were:

Engine thrust scale factor,	*Wing planform area,*
Wing trailing edge sweep,	*Wing aspect ratio,*
Wing thickness/chord ratios,	*Fuel tank size,*
Lift-off speed,	*Throttle cutback height,*
Angle of attack on approach,	*Altitude at start of cruise-climbs.*

The Mid-Tandem Fan (MTF) variable cycle engine was considered appropriate for the study since it is one of the more promising concepts identified to date[6]. It is able to limit airfield noise by changing its cycle at low speed to give reduced jet velocities. The engine used for the study was designed for a cruise speed of Mach 2.0 and had its nozzle exit jet velocity at take-off restricted to 400m/s to limit noise. A technology standard considered

representative of the near future was used within the engine, including a maximum continuous compressor delivery temperature (T_3) of 950K and a maximum continuous stator outlet temperature of 1750K (Olympus values are 850K and 1410K respectively).

The fuselage structure of the study SCT assumed a 20% mass reduction relative to Concorde due to improved manufacturing and Aluminium alloys, and a further 10% reduction due to the conservative use of composites. The wing structure assumed similar reductions through the use of Titanium and composites. A factor was applied to the fuselage mass of the study aircraft to represent an higher stiffness requirement relative to Concorde, due to increased fuselage slenderness.

The study assumed that only limited area-ruling of the fuselage would be used, and in particular that the passenger cabin width did not narrow to less than six abreast seating, except at the very front and back as part of the nose and tail tapers. Simple leading and trailing edge flaps, each of approximately 8% gross wing area, were assumed to be present. The leading edge flaps were used on take-off and in subsonic cruise for drag reduction, while the trailing edge flaps were only deployed during the approach to provide additional lift.

Baseline Configuration and Noise Limit Sensitivities

The optimised Stage 3 configuration obtained from ASTRO is summarised in table 1. This shows that the approach noise is the only active noise constraint, being the maximum allowed 2 EPNdB above its limit. Sideline and flyover noise are both well below their respective limits so throttle cutback height is not strongly driven in a particular direction and takes an arbitrary value.

ASTRO was then run as for the baseline case, except that one of the three noise limits was reduced relative to its Stage 3 value, while the remaining two limits were kept at their Stage 3 values. The rules governing the application of the limits were not changed. The sensitivities of the optimum configuration to changes in individual noise limits were thus obtained, and these results are shown in figure 3 for all three limits. The curves in figure 3 were all continued to the lowest noise limit at which a solution could be determined.

Approach noise limit sensitivity. As indicated above the baseline configuration suffers from high approach noise. Approach speed is also at its maximum permitted value, indicating that all scope for reducing approach noise by increasing speed has been exhausted. Figure 3 contains the approach noise limit sensitivity curve, which shows the variation of the take-off mass of the optimised aircraft as the approach noise limit is varied relative to its Stage 3 value. The right hand end of the curve is flat, indicating that when the approach noise limit is high enough the noise requirements are easily met and do not drive the design. The steeply climbing left hand end of the curve is where the approach noise limit has been reduced sufficiently to force design changes to be made to the aircraft to enable it to continue meeting the noise requirements. These design changes incur the mass penalties shown. It can be seen that the baseline configuration lies on the steep part of the curve, and has incurred a take-off mass penalty of about 2 tonnes in order to meet the Stage 3 approach noise limit.

Parameter	Optimised value
Fuselage length	89.0 m *
Gross wing area	1089 m^2
Gross wing aspect ratio	2.412
Max. thrust per engine (SL, static)	332.6 kN
Minimum lift-off speed	103.4 m/s
Lift-off speed used	103.4 m/s
Throttle cutback height	173.2 m
Flyover height	313.6 m
Approach speed	82.3 m/s
Approach angle-of attack	8.17 deg.
Sideline noise: estimated	99.1 EPNdB
limit	103.0 EPNdB
(limit exceedance)	-3.9 EPNdB
Flyover noise: estimated	104.4 EPNdB
limit	106.0 EPNdB
(limit exceedance)	-1.6 EPNdB
Approach noise: estimated	107.0 EPNdB
limit	105.0 EPNdB
(limit exceedance)	+2.0 EPNdB
Operating mass empty	166200 kg
Payload mass	24040 kg *
Fuel mass	209000 kg
Take-off mass	397200 kg

* Fixed value, does not change during optimisation.

TABLE 1: Optimised Stage 3 SCT configuration

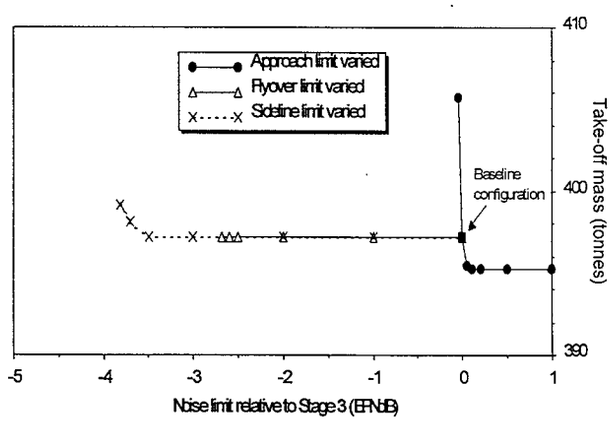

FIGURE 3: Datum SCT noise limit sensitivities

Flyover noise limit sensitivity. Table 1 shows that the flyover and sideline noise levels of the baseline configuration are well below their respective Stage 3 limits. Figure 3 demonstrates that the flyover noise limit can be reduced by -2.7 EPNdB relative to its Stage 3

value before solutions for the study aircraft become impossible. Reduction of the relative flyover noise limit below -2.7 EPNdB cannot be accommodated by reducing the flyover noise of the study aircraft as the necessary design changes would violate constraints that are already active. In particular the baseline configuration is only just able to satisfy the Stage 3 approach noise limit, which prevents the use of design changes that adversely affect approach noise by even a small amount. The aircraft take-off mass is above the threshold of 386 tonnes at which the Stage 3 flyover noise limit ceases to rise with take-off mass, and hence there is no scope to ease the flyover noise constraint by increasing aircraft mass.

Sideline noise limit sensitivity. The noise constraint requiring the sum of the three noise limit exceedance margins (positive when exceeding the limit and negative when satisfying it) to be zero or less is easily met by the baseline configuration. This is largely due to the substantial negative exceedance margin of -3.9 EPNdB for the sideline noise shown in table 1. However, this margin is eroded as the sideline noise limit is reduced relative to its Stage 3 value, until the sum of the three exceedances rises to zero and the relevant constraint becomes active. This occurs for the study aircraft at a relative sideline noise limit of -3.5 EPNdB. Further reduction of the relative sideline noise limit below -3.5 EPNdB can only be accommodated by design changes which reduce sideline noise, but which also incur the increase in take-off mass shown in figure 3. It is noticeable that solutions cannot be found once take-off mass approaches 400 tonnes, which is the point at which the Stage 3 sideline noise limit stops rising with mass. Detailed examination of the results confirmed that as take-off mass approaches 400 tonnes the increase in the Stage 3 noise limit partly counters reductions relative to that limit, enabling further solutions to be found.

Noise Reduction Studies

Following establishment of the datum noise limit sensitivities, several measures were investigated which were considered to have noise reduction potential.

Increased Glideslope Angle

Increasing the approach glideslope angle above the normal three degrees was considered as a method of approach noise reduction. This places the aircraft higher above the noise measurement point, although the safety, comfort and undercarriage mass implications of increased sink rates might militate against such a solution; and compatibility with other air traffic could also be a problem.

Glideslope angles of 3.5 and 4.0 degrees were investigated and new approach noise limit sensitivities calculated. Figure 4 shows these together with the original sensitivity curve. A simple inverse square reduction in approach sound pressure level with height above the approach noise measurement point was assumed, which gives a 2.2 EPNdB reduction in approach noise for a fixed aircraft at a fixed throttle setting, when glideslope angle is increased from three to four degrees. Comparison of the curves in figure 4 reveals that such a glideslope change reduces the approach noise of the optimised aircraft by about 3.0 EPNdB, which comprises the 2.2 EPNdB due to increased height and a further 0.8 EPNdB due to reductions in the approach thrust requirement. An increase in glideslope angle of half a degree allows the optimised aircraft to accommodate a 1.6 EPNdB reduction in the approach noise limit.

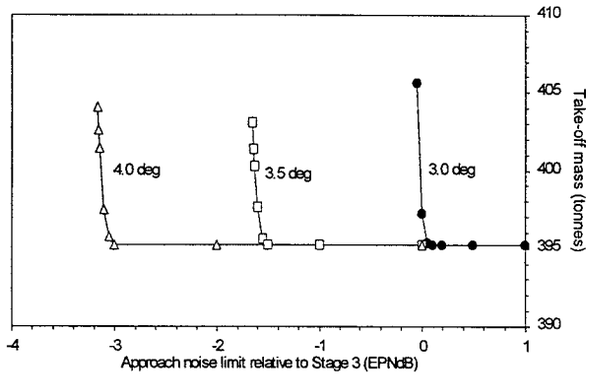

FIGURE 4: Effect of glideslope angle on SCT approach noise limit sensitivity

Low-speed Drag Reduction

A 5% reduction in total aircraft drag at low speed ($0 \leq Mach \leq 0.4$) was introduced, and a new set of noise limit sensitivity curves produced. These are shown plotted in figure 5, superimposed on the datum curves.

Approach noise limit sensitivity with reduced low-speed drag. With reduced low-speed drag the thrust required on approach decreases, resulting in reduced approach noise. Consequently the optimum configuration with Stage 3 noise limits applied no longer has an active approach noise constraint, and its take-off mass is 2 tonnes less than the baseline case. However, figure 5 shows that even with a 5% low-speed drag reduction the relative approach noise limit can only be reduced to -0.2 EPNdB before the approach noise constraint of the study aircraft becomes active again and the take-off mass starts to climb steeply once more.

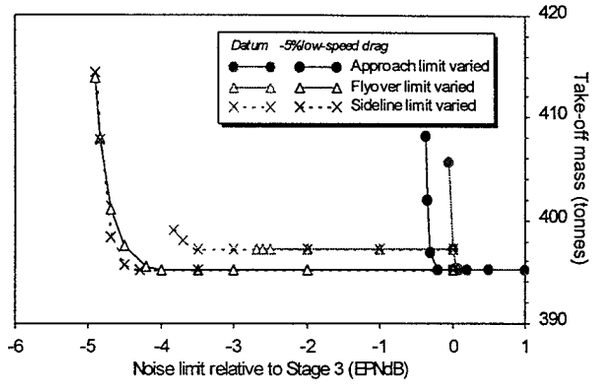

FIGURE 5: The effect of low-speed drag reduction on noise limit sensitivities

Flyover noise limit sensitivity with reduced low-speed drag. The low-speed drag reduction also reduces the thrust required after throttle cutback and hence reduces the flyover noise. This noise reduction allows the flyover noise limit to be reduced to -4.0 EPNdB relative to its Stage 3 value before the sum of positive noise limit exceedances for the study aircraft reaches the maximum value of 3 EPNdB permitted under Stage 3 rules. If the relative flyover noise limit is reduced below -4.0 EPNdB then design changes which decrease noise but also increase take-off mass become necessary. Some of these design changes and their effect on flyover height and thrust are shown in figure 6. The associated mass rise becomes very steep, as shown in figure 5, so that the aircraft mass soon becomes too high for all constraints to be met and no further solutions can be found.

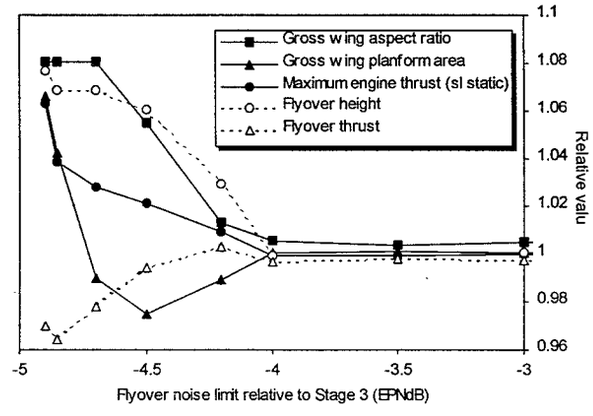

FIGURE 6: Variation of key parameters with flyover noise limit (with 5% low-speed drag reduction)

Sideline noise limit sensitivity with reduced low-speed drag. A reduction in low-speed drag does not necessarily reduce sideline noise since the latter is normally determined by an aircraft's maximum thrust, which is used during take-off and up to the throttle cutback height. For a given throttle cutback height the sideline noise will therefore only be reduced if engine size is reduced. With Stage 3 noise limits applied no significant change in engine size, and hence sideline noise, was obtained when low-speed drag was reduced by 5%.

Figure 5 shows that, with the 5% low-speed drag reduction, the sideline noise limit can be reduced by -4.3 EPNdB relative to its Stage 3 value before the study aircraft incurs design changes which cause a mass increase. During this reduction of the sideline limit the sideline noise of the study aircraft remains roughly constant, causing the excess sideline noise, which is initially negative, to rise. The sum of all three noise limit exceedances reaches its maximum permitted value of zero when the relative sideline noise limit has been decreased to -4.3 EPNdB. This is 0.8 EPNdB lower than the point at which the same situation occurred with the datum drag. This difference is due to the reduced flyover noise with reduced low-speed drag, which reduces the excess flyover noise hence providing a larger margin by which the excess sideline noise can rise. Hence reduced flyover noise can be used to accommodate reductions in the sideline noise limit.

Cruise Drag Reduction

5% reductions in subsonic ($0.90 \leq Mach \leq 0.98$) and supersonic ($1.9 \leq Mach \leq 2.1$) cruise drag values were separately introduced, and new sets of noise limit sensitivities obtained in each case. These are shown plotted in figure 7, together with the datum sensitivities.

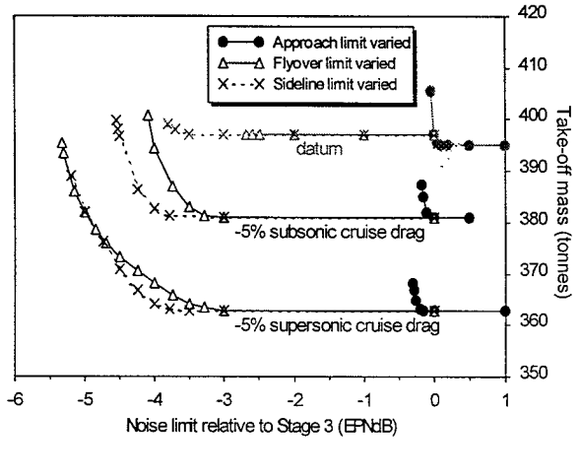

FIGURE 7: The effects of cruise drag reductions on noise limit sensitivities

For a fixed aircraft design a reduction in cruise drag reduces the cruise thrust requirements and, over the length of the mission, a significant reduction in the total fuel required can result. If the aircraft design is also re-optimised (take-off mass being minimised) to take full advantage then significant reductions in aircraft empty mass can be obtained. Hence relatively small reductions in cruise drag can result in substantial take-off mass reductions. Figure 7 shows that when all noise

constraints are inactive (above a relative noise limit of +0.1 EPNdB for all cases) reducing the subsonic cruise drag by 5% reduces take-off mass by about 3.6% while reducing the supersonic cruise drag by 5% reduces take-off mass by about 8.2%. The difference between these mass reductions is partly due to the difference between the subsonic and supersonic leg lengths.

Approach noise limit sensitivity with reduced cruise drag. If the three approach noise limit curves in figure 7 are compared, they appear similar except for their vertical separation. In each case the steep rise in take-off mass is caused by design changes triggered by the excess approach noise and the approach speed both being at their maximum permitted values. The point at which this first occurs, as the relative approach noise limit is reduced, differs slightly for each case due to their differing configurations.

Flyover noise limit sensitivity with reduced cruise drag. Figure 7 shows that with a 5% reduction in either subsonic or supersonic cruise drag the flyover noise limit can be reduced by about 3.0 EPNdB relative to the Stage 3 limit without provoking design changes which incur a mass penalty. This is only slightly lower than the relative flyover limit that could be reached in the datum case. However, with reduced cruise drag the optimum designs are not as tightly restricted by active approach noise and speed constraints, and significant further reductions of the relative flyover noise limit below -3.0 EPNdB can be accommodated through design changes.

Sideline noise limit sensitivity with reduced cruise drag. If the sideline noise limit is reduced relative to its Stage 3 value the sideline noise of the study aircraft initially remains unchanged causing its excess sideline noise, which is initially negative, to increase. This occurs in the datum and reduced cruise drag cases shown in figure 7, and in all three cases the rise in excess sideline noise causes the sum of all three noise limit exceedances to reach its maximum permitted value of zero at a relative sideline noise limit of about -3.5 EPNdB.

To accommodate further reductions of the sideline noise limit, design changes incurring mass increases are necessary. As figure 7 shows, the datum drag case can only incur a slight mass increase before it becomes impossible to find a solution that achieves the required aircraft performance. However, the reduced cruise drag cases have initially lower take-off masses and so can incur greater mass increases, to accommodate greater reductions of the sideline noise limit, before their mass becomes high enough to prevent satisfaction of the performance requirements.

Noise Reduction Studies Using Flap Systems

Concorde did not use any flap systems, its trailing-edge elevons being for trim and control purposes only. It relied on vortex flow to reduce incidence but its subsonic performance suffered as a result. The next generation of SCT aircraft will need to improve its low speed performance by the use of flaps[7]. The flaps are envisaged as plain hinged surfaces on the leading-edge and on the trailing-edge by utilising the existing elevon control surfaces. Leading-edge (LE) flaps reduce separation and suppress vortex flow, thus reducing lift but increasing aerodynamic performance in terms of lift/drag ratio. The elevons being used as trailing-edge (TE) flaps increase lift but also reduce separation at the leading-edge as a result of reducing incidence. These effects have been modelled within ASTRO at both subsonic cruise and low speed conditions.

The problem with TE devices is the large pitching moments which need to be trimmed. The use of a foreplane or tailplane, along with relaxed longitudinal stability, provide solutions but these effects along with the control power requirements are not currently modelled by ASTRO. More detailed studies of the low speed trim and control requirements of a typical SCT have validated the use of TE devices within the ASTRO low speed performance estimation but that the extent of their deflection may need to be limited.

Initial runs of ASTRO for the study aircraft revealed that in the absence of TE device deflection, significant increases in wing area, and hence aircraft mass and drag, were necessary to obtain sufficient lift to achieve the approach speed. Hence the baseline aircraft studied above assumed the LE flaps were not deployed on approach in order not to lose lift and TE devices were set at an optimum deflection up to 15 degrees.

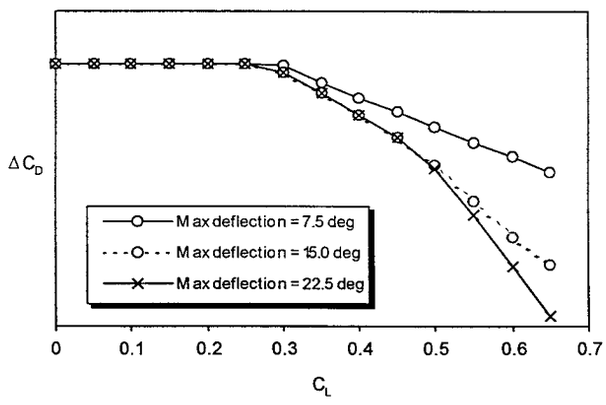

FIGURE 8: Trailing-edge flap standards

A study was therefore undertaken into different levels of TE flap deflection, to investigate their effect on the configuration and the net noise benefits that might result.

The TE deflection angles were all optimum settings to give minimum drag at any given CL, but differed in the allowable maximum setting. Figure 8 shows the differences in drag of the various flap standards relative to zero TE flaps.

Baseline Configuration

In the preceding studies optimum TE flap deflections of up to 15 degrees were used, allowing optimised solutions to be obtained for the original baseline configuration. For the purposes of this flap study, a new baseline configuration was defined with an easier set of performance requirements such that a viable solution could be achieved without the need for TE flap deflection. Note that the TE devices still exist on all configurations because of their use as elevon control surfaces. The optimised aircraft was required to achieve the following performance (only differences from the previous baseline are specified):

- *Accommodate 200 passengers in 5 abreast seating,*
- *Fly a range of 5500nm, of which the first 3700nm is flown at Mach 2.0 and the final 1800nm is flown at Mach 0.95, with a full passenger load,*
- *A minimum climb capability in cruise of 1.52m/s (300ft/min).*

The optimised stage 3 configuration obtained from ASTRO is summarised in table 2.

Parameter		Optimised value	
Fuselage length		89.0 m	*
Gross wing area		956 m^2	
Gross wing aspect ratio		2.046	
Max. thrust per engine (SL, static)		251.5 kN	
Minimum lift-off speed		100.0 m/s	
Lift-off speed used		102.0 m/s	
Throttle cutback height		150.0 m	
Flyover height		277.6 m	
Approach speed		82.3 m/s	
Approach angle-of attack		11.0 deg.	
Sideline noise:	estimated	97.5 EPNdB	
	limit	102.0 EPNdB	
	(limit exceedance)	-4.5 EPNdB	
Flyover noise:	estimated	105.1 EPNdB	
	limit	104.7 EPNdB	
	(limit exceedance)	+0.4 EPNdB	
Approach noise:	estimated	107.0 EPNdB	
	limit	105.0 EPNdB	
	(limit exceedance)	+2.0 EPNdB	
Operating mass empty		126800 kg	
Payload mass		19000 kg	*
Fuel mass		164400 kg	
Take-off mass		308700 kg	

* Fixed value, does not change during optimisation.

TABLE 2: Optimised Stage 3 SCT - New baseline

The approach angle of attack is on its upper limit of 11 degrees showing that the approach speed is an active constraint and is driving the size of the wing area. The approach noise is the only active noise constraint although flyover noise also exceeds its limit.

Datum noise limit sensitivities. The sensitivities of the optimum baseline configuration with zero TE flap deflection to changes in individual noise limits were obtained as before and the results are shown in figure 9. The right hand ends of the sensitivity curves are flat indicating the noise requirements do not drive the design of the baseline configuration. However, the approach noise sensitivity curve rapidly rises such that viable solutions became impossible after only slight reductions in the relative noise limit. The optimum configuration design is not so sensitive to changes in flyover and sideline noise limits although design changes are necessary after -1 EPNdB and -2 EPNdB limit reductions respectively. Further noise limit reductions are possible by increasing wing area and aspect ratio. The rise in take-off mass is more gradual due to the take-off mass being much lower than the mass thresholds of the Stage 3 limit.

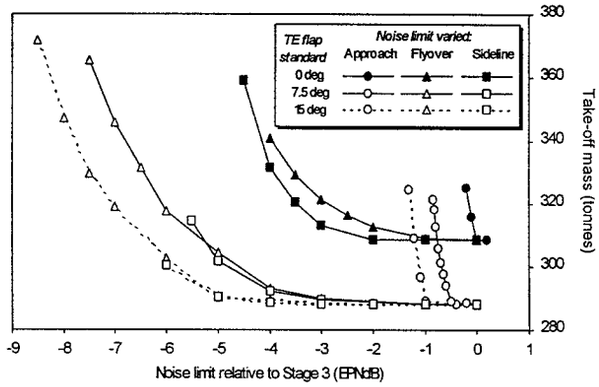

FIGURE 9: The effect of TE flap deflection on noise limit sensitivities

Effect of Trailing-edge Flap Deflection

The optimum Stage 3 configuration with TE flaps deflected was found to have a 6.6% (~20 tonnes) reduced maximum take-off mass compared to the baseline. Additional TE flap deflection above the 7.5 degree standard did not change this optimum design as shown in figure 9. The TE flaps at this level had provided sufficient lift on approach such that the approach speed constraint was no longer driving the wing area. Other constraints such as fuel volume now defined the minimum wing area, allowing an 18% decrease in size. Increasing TE flap deflection did continue to reduce approach noise due to a reduction in the required approach thrust, facilitated by keeping approach speed high through reduced incidence.

Noise limit sensitivities with TE flap deflection. Figure 9 shows the noise sensitivity curves with both the 7.5 degree and 15 degree standard flaps deployed together with the datum sensitivities. The approach noise sensitivities appear similar to those found for the low speed drag reduction, apart from the vertical separation. This is not surprising because the TE flaps have effectively reduced the low speed drag at the approach flight condition and the vertical separation is due to the change in wing sizing constraints from the additional benefit of increased lift. The steep mass rise has been delayed by -0.5 EPNdB and -1.0 EPNdB for 7.5 and 15 degree TE flap standards respectively. This shows the changes in drag due to the flap deployment are larger than the 5% assumed in the low speed drag reduction study which delayed the mass rise by -0.3 EPNdB. The use of the 22.5 degree standard flaps did not improve the optimum configurations any further than the 15 degree standard. This is because the levels of CL used are below those where 22.5 degree deflection becomes optimum for drag as shown in figure 8.

The flyover sensitivity curves show similar variations with TE flap standard as for the approach. Sudden mass rises do not occur but for a given take-off mass, flyover noise limit can be reduced by about 3 EPNdB with 7.5 degrees flap standard and by a further 1 EPNdB with 15 degrees. The above include the changes due to the vertical step in take-off mass.

Effect of Leading-edge Flap Deflection on Approach

So far it has been assumed that LE flaps have not been deployed during approach, in order to maximise lift. However, with TE flaps providing scope for changing lift, LE flaps may be advantageous in reducing drag. Figure 10 shows the effect on the approach noise limit sensitivities with LE flaps deflected in combination with zero and 15 degree TE flap standards. With zero TE flaps the optimum Stage 3 configuration has a mass penalty of over 50 tonnes due to the increased wing area needed to meet the approach speed. However, the reduction in low speed drag does allow the approach noise limit to be reduced by 2 EPNdB whilst still achieving viable configurations.

As long as there is sufficient TE flap deflection to achieve approach speed constraints without affecting the wing area, then deployment of LE flaps during approach will not penalise take-off mass. Figure 10 shows that in this case, LE flaps will allow much greater reductions (2 EPNdB) in approach noise limits before mass penalties are incurred. The rise in mass is also less steep due to the increased flexibility of the design to constraints.

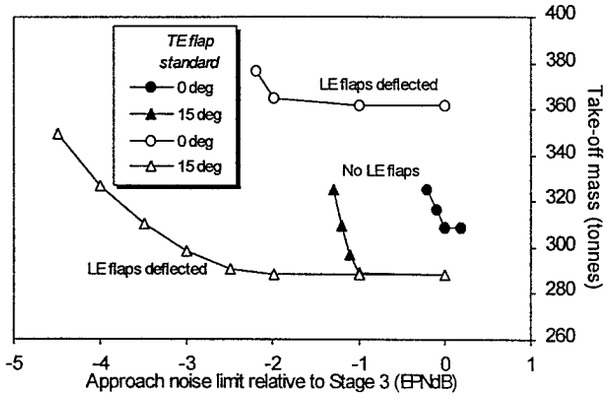

FIGURE 10: The effect of LE flap deflection on approach noise limit sensitivity

Optimisation of Initial Climb Speed

In some cases it was found that the engines of the optimised aircraft were being sized to achieve the specified initial climb speed (V_{ic}), which was set at 250 knots EAS throughout these studies. This value is the maximum normally allowed around airports, to ease air traffic control. The matter was investigated further to establish whether optimising this speed might produce useful mass or noise benefits for an SCT.

With the datum SCT configuration (253 seat, 6 abreast, 5700nm range) no mass reductions were obtained when V_{ic} was reduced, but a mass increase occurred if it was increased, suggesting that V_{ic}=250kts gives a minimum mass solution for this particular aircraft. However, when the emphasis between range and payload was altered then the minimum mass value of V_{ic} also changed. With a different configuration with an extended range and reduced payload (225 seat, 5 abreast, 6000nm range), but otherwise using the same engine and assumptions, the use of V_{ic}=250kts was found to incur the mass penalty apparent in figure 11. The take-off mass of this aircraft can be reduced by 3% (~11 tonnes) if V_{ic} is reduced to 240kts or less.

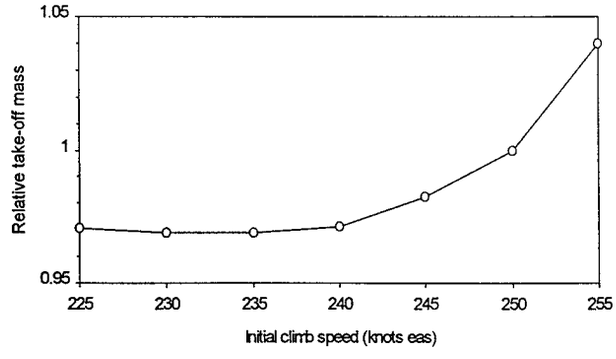

FIGURE 11: The effect of initial climb speed on take-off mass

The mass penalties incurred when using values of V_{ic} above 240kts come from the need to use higher lift-off speeds (an independent variable in ASTRO), as shown in figure 12, in order to achieve the higher initial climb speeds. Since additional horizontal distance is not available to accelerate to higher lift-off speeds, engine size must be increased to improve acceleration as shown in figure 13. This oversizes the engine for the remainder of the mission, resulting in the take-off mass penalties. It is interesting to note that the variation of the two wing parameters shown in figure 13 does not alter the wing mass, but shows a shift in optimum planform with changing engine size and take-off mass. Oversized engines have a particularly adverse effect on supersonic cruise drag and the reduction in wing aspect ratio with increasing engine size indicates an attempt by ASTRO to partly offset this by improving the wing for this regime.

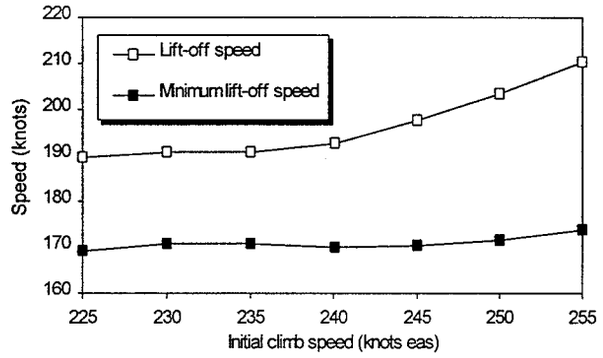

FIGURE 12: Variation of lift-off speed with initial climb speed

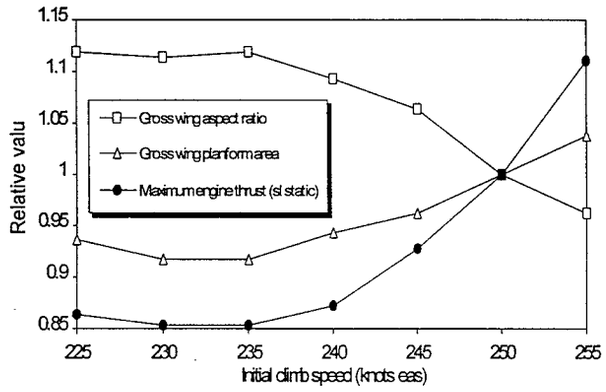

FIGURE 13: Variation of key design parameters with initial climb speed

Altering the initial climb speed of the 225 seat, 6000nm range SCT also changes its airfield noise levels as shown in figure 14. None of the noise constraints were active for this aircraft when meeting Stage 3 noise limits and so the throttle cutback height was not driven to a particular value and remained constant for all values of V_{ic}. Consequently as V_{ic} is reduced, and engine size falls, so the sideline noise also falls since in ASTRO this noise level is determined by maximum available thrust and cutback height only.

The reductions in lift-off speed and engine thrust with V_{ic} result in significantly lower flyover heights being achieved, which increases the flyover noise as also shown in figure 14. The increases in flyover noise are greater than the reductions in sideline noise, while approach noise remains fairly constant. Reducing the initial climb speed of this aircraft therefore increases the sum of the excess noise levels.

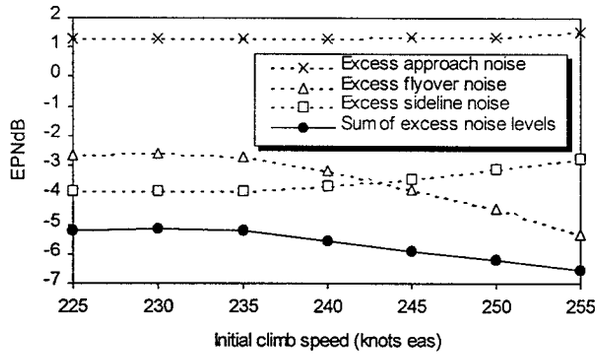

FIGURE 14: Effect of reduced initial climb speed on aircraft noise

Conclusions

The methodology and modelling of the ASTRO multivariate optimisation code have been described. The performance aspects most critical to SCT viability have been incorporated, notably including airfield noise prediction which can be used to drive the design to satisfy specified noise regulations. This capability is demonstrated by the presented noise-related studies.

A minimum take-off mass SCT aircraft meeting Stage 3 noise requirements was obtained. However, large mass penalties were incurred when overall aircraft redesign became necessary to accommodate reduced noise limits. The Stage 3 approach noise limit could only be met by the study aircraft by incorporating design changes which resulted in a 2 tonne mass penalty. No significant reduction of the approach noise limit below its Stage 3 value could be accommodated without the use of new technologies or measures.

Increased glideslope angle was shown to be an effective way of reducing approach noise, a 0.5 degree increase accommodating a 1.6 EPNdB reduction in the approach noise limit. However, concerns over the safety and practicality of such a measure need to be explored further.

Drag reduction is an essential part of the aircraft design process and has been shown to offer potential benefits to airfield noise. Low-speed drag reduction directly reduces approach and flyover noise through reduced thrust requirements, and these reductions can be used to accommodate useful reductions in any of the three noise limits, due to the flexibility of the noise limit application rules. A 5% reduction in low-speed drag at constant take-off mass allowed reductions in approach/flyover/sideline noise limits of about 0.3/1.8/1.1 EPNdB respectively, relative to the datum cases. The precise noise benefits of drag reductions depend on whether the designer is willing to trade increased take-off mass for reduced noise. This is particularly true of cruise drag reductions. For example, for the study aircraft with a 5% reduction in supersonic cruise drag, a reduction of the relative flyover noise limit from -3 to -5.3 EPNdB can be accommodated at the cost of a mass increase of 30 tonnes. The resulting take-off mass would still be no greater than that of the baseline aircraft since the mass increase has simply eroded the mass reduction obtained from the cruise drag reduction.

The use of TE flaps to provide extra lift was shown to provide significant reductions in take-off mass but can also allow the use of LE flaps on approach. Both flap systems allowed reductions in all noise limits but LE flaps offered the greatest potential. The critical approach noise limit could be reduced by about 1 EPNdB using optimum TE flaps and by a further 1.5 EPNdB by additional LE flap deflection without incurring any mass penalties.

Optimisation of initial climb speed was found to offer useful reductions in take-off mass in some circumstances. However this was achieved at the cost of increased flyover noise, partly countered by a smaller reduction in sideline noise, and so is only beneficial where noise constraints allow.

The studies presented in this paper have illustrated a number of the complex interactions which occur between design variables and performance parameters. The use of constraint sensitivity curves has shown the importance of identifying the potential mass penalties due to particular constraints and hence indicate where procedure or technology improvements should be applied

Acknowledgements

The DERA part of the presented work has been funded by the United Kingdom Department of Trade and Industry, under the CARAD programme.

References

1. Lovell, D.A., 'Some experiences with numerical optimization in aircraft specification and preliminary design', Proceedings of 12th Congress ICAS, Munich, October 1980.
2. Smith, J., Lee, C., 'The RAE combat aircraft multi-variate optimisation method', AIAA Paper 89-2080, 1989.
3. Kirk, J.A., 'The use of multivariate analysis to optimise design parameters for extended-range combat aircraft', AIAA Paper 92-4707, 1992.
4. Hutchison, M.G., et al., 'Variable-complexity aerodynamic optimization of an HSCT wing using structural wing-weight equations', AIAA Paper 92-0212, January 1992.
5. Raymer, D.P., 'Aircraft Design: A Conceptual Approach', AIAA Education Series, 1989.
6. Hodder, S.D., 'A comparison of possible powerplants for a second generation supersonic transport aircraft', Proceedings of EAC'94, 7th European Aerospace Conference, Toulouse, 25-27 October 1994.
7. Nicholls, K.P., 'Flap Systems on Supersonic Transport Aircraft', Proceedings of 20th Congress ICAS, Sorrento, September 1996.